Subcellular Metabolite Transport and Carbon Isotope Kinetics in the Intramyocardial Glutamate Pool[†]

Xin Yu, Lawrence T. White, Nathaniel M. Alpert, and E. Douglas Lewandowski*

NMR Center, Department of Radiology, Massachusetts General Hospital and Harvard Medical School, Boston, Massachusetts 02129

Received January 26, 1996; Revised Manuscript Received March 18, 1996[⊗]

ABSTRACT: The pathophysiological state of the cell must be translated into the mitochondria to meet the demands for oxidative energy production. Metabolite exchange across the mitochondrial membrane provides this communication and was observed with ^{13}C NMR spectroscopy of hearts oxidizing [2-^{13}C]-butyrate at normal or high cytosolic redox state. Previous NMR observations of ^{13}C turnover within the glutamate pool of intact tissues have indicated its relationship with metabolic flux through the tricarboxylic acid (TCA) cycle, but the direct influence of isotope exchange between the TCA cycle intermediates in the mitochondria and the cytosolic glutamate pool has been much less considered. This current study was designed to determine whether the physical transport of metabolites across the mitochondrial membrane of intact heart tissues could be discerned as a rate determinant for isotope turnover in the NMR-detectable glutamate pool. ^{13}C entry into glutamate provided measures of TCA cycle flux and the interconversion between mitochondrial intermediates and cytosolic glutamate. The influence of the malate−aspartate shuttle activity was examined by comparing two groups of hearts: one group oxidizing 2.5 mM [2-^{13}C]-butyrate ($n = 5$) and the other oxidizing 2.5 mM [2-^{13}C]butyrate in the presence of a lactate (2.5 mM)-induced elevation in the cytosolic redox to stimulate shuttle activity ($n = 5$). High redox state did not affect TCA cycle flux but increased the rate of interconversion between α-ketoglutarate and glutamate from 3.1 ± 0.2 μmol min^{-1} (g dry)$^{-1}$ to 14.3 ± 2.0. High resolution ^{13}C NMR spectra of tissue extracts confirmed that the exogenous lactate did not contribute as a carbon source for the formation of either the TCA cycle intermediates or glutamate. In both groups, over 95% of the acetyl-CoA was derived from the short-chain fatty acid butyrate, irrespective of the presence of lactate. Additional hearts perfused with unlabeled butyrate and [3-^{13}C]lactate showed no label entry into glutamate, but rather the formation of [3-^{13}C]alanine, indicating the net reverse flux through lactate dehydrogenase to increase NADH production. Thus, the addition of lactate served only to augment cytosolic redox state to drive the malate−aspartate shuttle. The dynamic-mode acquisition of ^{13}C NMR data from intact hearts, oxidizing [2-^{13}C]-butyrate with or without additional lactate, demonstrated the influence of malate−aspartate shuttle activity on the ^{13}C enrichment rates within glutamate. These data indicate metabolic communication between the mitochondria and cytosol in response to the physiological state of intact tissues.

Physical compartmentation of metabolism in living cells is important for regulating energy production in coordination with cell function. Adapting the energy-yielding, intermediary metabolism of mitochondria to existing functional or pathophysiological states can be accomplished through adjustments in the balance of metabolic intermediates exchanging between the mitochondria and cytosol (LaNoue & Williamson, 1971; Lewandowski et al., 1995; Safer, 1975). The malate−aspartate shuttle is a direct link between the cytosolic and mitochondrial metabolites and serves the function of transferring reducing equivalents from the cytosol to the electron transport chain of the inner mitochondrial membrane (Safer, 1975). In the process, TCA cycle[1] intermediates exchange with cytosolic metabolites through carrier mediated transport involving the glutamate/aspartate exchanger and the α-ketoglutarate/malate exchanger (LaNoue & Williamson, 1971). However, this exchange has only been studied in isolated mitochondria with artificial cytosolic environments. The opportunity to examine subcellular metabolite exchange in intact tissues with carbon-13 (^{13}C) NMR spectroscopy opens a new window for observing physiochemical regulation and metabolic communication between the mitochondria and cytosol.

Pre-steady-state incorporation of ^{13}C into the tissue glutamate pool is related to oxidative metabolic flux through the TCA cycle (Chance et al., 1983; Lewandowski, 1992; Robitaille et al., 1993; Weiss et al., 1992), but is also known to depend on the exchange of label between the TCA cycle intermediates and glutamate (Randle et al., 1970; Weiss et al., 1995, Yu et al., 1995). Collection of such dynamic-mode NMR data from intact tissues relies heavily on the

[†]This work was supported by National Heart, Lung, and Blood Institute Grant RO1HL49244 (E.D.L.) and was done during the tenure of an Established Investigator Award from the American Heart Association to E.D.L.

* Address for correspondence: E. Douglas Lewandowski, Ph.D., NMR Center, Massachusetts General Hospital, Bldg. 149, 13th St., Charlestown, MA 02129. Tel: (617) 726-5639; Fax: (617) 726-7422.

[⊗] Abstract published in *Advance ACS Abstracts,* May 1, 1996.

[1] Abbreviations: NMR, nuclear magnetic resonance; GOT, glutamate−oxaloacetate transaminase; ATA, alanine transaminase; TCA cycle, tricarboxylic acid cycle; V_{TCA}, measured tricarboxylic acid cycle flux; F_1, interconversion rate between α-ketoglutarate and glutamate; NAD, nicotinamide adenine dinucleotide.

S0006-2960(96)00199-7 CCC: $12.00

labeling of the NMR-observable glutamate pool, which is 90% cytosolic in mammalian hearts (LaNoue et al., 1970; Yu et al., 1995). Thus, exchange of isotope between the TCA cycle intermediates within the mitochondria and the cytosolic glutamate pool involves not only chemical interconversion but also metabolite transport across the mitochondrial membrane. Previous work, comparing isotope exchange rates to flux through the enzyme, cardiac glutamate−oxaloacetate transaminase (GOT), demonstrated that the actual interconversion of α-ketoglutarate and glutamate was 20-fold slower than GOT flux (Yu et al., 1995). This discrepancy suggests that metabolite transport is a rate-determining step in ^{13}C enrichment of the glutamate pool.

In the present study, ^{13}C turnover within the glutamate pool of perfused rabbit hearts was observed with ^{13}C NMR spectroscopy at augmented cytosolic redox state (NADH/NAD^+) induced by exogenous lactate (Scholz et al., 1995). Changing the cytosolic redox state during ^{13}C enrichment of the intramyocardial glutamate pool allowed us to determine whether ^{13}C NMR observations of intact, functioning organs are sensitive to redox-dependent transport activity via the malate−aspartate shuttle. The results indicate that the rates of this subcellular metabolite exchange do respond to the physiological state of the cell and that such observations are now possible from intact tissues via ^{13}C NMR spectroscopy.

MATERIALS AND METHODS

Isolated Heart Preparation. Use of animals conformed to the guiding principles established by Massachusetts General Hospital. Rabbits were heparinized (1000 units) and anesthetized (sodium pentobarbital, 100 mg/kg ip). The heart was excised and cannulated for retrograde perfusion at 100 cm hydrostatic pressure with a modified Krebs−Henseleit buffer equilibrated with 95% O_2−5% CO_2 at 37 °C. Perfusate was recirculated from a 450 mL reservoir. Contractile function was continuously monitored using a fluid-filled, latex balloon inside the left ventricle and connected to a pressure transducer line and physiograph (Gould, Inc., Cleveland, OH). Myocardial oxygen consumption was determined from the difference in O_2 content of perfusate in the arterial supply at the aortic cannula and coronary effluent from the pulmonary artery (Neely et al., 1967).

Experimental Protocols. Isolated hearts were perfused with ^{13}C-enriched butyrate, a short chain fatty acid which undergoes β-oxidation without the confounding factors of activation and membrane transport of long chain fatty acids. Prior to the delivery of media containing ^{13}C-enriched substrate, the corresponding unlabeled substrate with or without lactate was introduced for 10 min to ensure that metabolic equilibrium was attained (Randle et al., 1970). The effect of adding lactate to the perfusion medium allowed comparison of ^{13}C kinetics from hearts at high (2.5 mM lactate) versus normal cytosolic redox state (no lactate) (Scholz et al., 1995). Each experimental group consisted of five hearts. As pyruvate dehydrogenase is inhibited in the presence of fatty acid oxidation (Dennis et al., 1979; Johnston & Lewandowski, 1991; Weiss et al., 1989), lactate did not contribute as a carbon source to oxidative metabolism. To document the metabolic fate of lactate, an additional heart was supplied with 2.5 mM unlabeled butyrate plus 2.5 mM [3-^{13}C] lactate. The role of lactate in this protocol was confirmed from the resulting ^{13}C NMR spectrum of the tissue extract.

NMR Spectroscopy. Hearts were situated in a 20 mm broadband NMR probe inside a 9.4 T vertical bore NMR magnet interfaced to a MSL 400 spectrometer (Bruker Instruments, Billerica, MA). Magnetic field homogeneity was optimized by shimming on the proton signal from water. ^{13}C NMR spectra were acquired from the intact heart at 101 MHz with a 45° pulse angle and 2 s recycle time over 64 scans with 8K data sets. Bilevel broadband decoupling was performed at 0.5 W (1.8 s) and 7.0 W (17 μs) without sample heating. During initial perfusion of the heart with unlabeled material, a natural abundance ^{13}C NMR spectrum was acquired. Upon delivery of ^{13}C-enriched substrate, ^{13}C spectra were acquired from the intact, functioning heart in 2 min time blocks. Natural abundance ^{13}C signal was subtracted and 20 Hz line broadening was applied to raw signal before being Fourier transformed into the frequency domain. NMR signal intensities were determined by Lorentzian curve-fitting and integrating the curve. At steady state isotope enrichment, hearts were freeze-clamped for biochemical assays (Williamson & Corkey, 1969; Yu et al., 1995) and *in vitro* ^{13}C NMR analysis (Lewandowski et al., 1991; Lewandowski, 1992; Malloy et al., 1988; Yu et al., 1995).

High-resolution ^{13}C NMR spectra of tissue extracts reconstituted in 0.5 mL of D_2O were collected with a 5 mm ^{13}C probe (Bruker Instruments, Billerica, MA) with a minimum of 6000 scans (45° pulse, 1.8 s recycle time) with broadband proton decoupling. The free induction decay was acquired with a 32K data set and zero filled to 64K to improve spectral resolution. The signal was processed by 1 Hz exponential filtering followed by Fourier transformation. High-resolution ^{13}C NMR spectra showed multiple labeling within the glutamate carbon chain, appearing as NMR signal splitting due to spin−spin coupling. Multiplet structure of these glutamate resonance peaks allowed determinations of the fractional enrichment of acetyl-CoA entering the citrate acid cycle (F_c) and the ratio of anaplerotic to citrate synthase flux (y) (Malloy et al., 1988). The results confirmed that only [2-^{13}C]butyrate, and no exogenous lactate, was oxidized through the TCA cycle.

Kinetic Measurements. The ^{13}C enrichment curves at the initial site of glutamate labeling, the 4-carbon, and the secondary enrichment site due to recycling of label by TCA cycle, the 2-carbon, were fit to a kinetic model. This model allowed the determination of both TCA cycle flux and the rate of interconversion between α-ketoglutarate and glutamate. The compartment model is based on flux through constant, measured metabolite pools and thus does not require measurements of oxygen consumption for determining TCA cycle flux. The kinetic model is described in greater detail in a previous report (Yu et al., 1995). The basic compartment model includes only rate-limiting TCA cycle intermediates (citrate, α-ketoglutarate, malate, and oxaloacetate) and amino acid pools that are in chemical exchange with the TCA cycle intermediates (glutamate and aspartate). By eliminating equations that describe the enrichment of the 3-carbon of glutamate, due to the symmetry of labeling at the 2- and 3-carbon sites, the model has nine compartments in total. Pre-steady-state ^{13}C enrichment of each metabolite at either the 4- or 2-carbon positions are then described by a set of nine differential equations. The equations describe the labeling history of the metabolites, by observing the principle

of mass conservation within the pools. The nine equations are as follows:

$$\frac{d}{dt}\text{CIT4} = \frac{V_{TCA}}{[\text{CIT}]}(F_c - \text{CIT4})$$

$$\frac{d}{dt}\alpha\text{KG4} = \frac{V_{TCA}}{[\alpha\text{KG}]}\text{CIT4} - \frac{V_{TCA} + F_1}{[\alpha\text{KG}]}\alpha\text{KG4} + \frac{F_1}{[\alpha\text{KG}]}\text{GLU4}$$

$$\frac{d}{dt}\text{GLU4} = \frac{F_1}{[\text{GLU}]}(\alpha\text{KG4} - \text{GLU4})$$

$$\frac{d}{dt}\text{CIT2} = \frac{V_{TCA}}{[\text{CIT}]}(\text{OAA2} - \text{CIT2})$$

$$\frac{d}{dt}\alpha\text{KG2} = \frac{V_{TCA}}{[\alpha\text{KG}]}\text{CIT2} - \frac{V_{TCA} + F_1}{[\alpha\text{KG}]}\alpha\text{KG2} + \frac{F_1}{[\alpha\text{KG}]}\text{GLU2}$$

$$\frac{d}{dt}\text{GLU2} = \frac{F_1}{[\text{GLU}]}(\alpha\text{KG2} - \text{GLU2})$$

$$\frac{d}{dt}\text{MAL2} = \frac{V_{TCA}}{[\text{MAL}]}[{}^1/_2\alpha\text{KG2} + {}^1/_2\alpha\text{KG4} - (1 + y)\text{MAL2}]$$

$$\frac{d}{dt}\text{OAA2} = \frac{V_{TCA}}{[\text{OAA}]}\text{MAL2} - \frac{V_{TCA} + F_2}{[\text{OAA}]}\text{OAA2} + \frac{F_2}{[\text{OAA}]}\text{ASP2}$$

$$\frac{d}{dt}\text{ASP2} = \frac{F_2}{[\text{ASP}]}(\text{OAA2} - \text{ASP2})$$

where CIT, αKG, GLU, MAL, OAA, and ASP are citrate, α-ketoglutarate, glutamate, malate, oxaloacetate, and aspartate, respectively. [CIT], [αKG], [GLU], [MAL], [OAA], and [ASP] are the total pool sizes of the corresponding metabolites. XXX*n* is the dimensionless fractional enrichment level of ^{13}C of a certain metabolite at the *n*th carbon position. F_1 and F_2 represent the interconversion rates, lumped to included both transamination and membrane transport, between α-ketoglutarate and glutamate, and between aspartate and oxaloacetate, respectively. Under the current experimental conditions where lactate did not directly contribute to the formation of oxidative intermediates, F_1 and F_2 are equal (Yu et al., 1995).

Rate-determining parameters in the model include TCA cycle flux (V_{TCA}), the interconversion rate between α-ketoglutarate and glutamate (F_1), and metabolite pool sizes. ^{13}C enrichment level of acetyl-CoA (F_c) and relative anaplerosis (y) were used as input parameters for ^{13}C enrichment level of each compartment. F_c and y were determined from *in vitro* ^{13}C NMR analysis (Malloy et al., 1988), and metabolite contents were measured by enzymatic assays (Williamson et al., 1976; Williamson & Corkey, 1969). TCA cycle flux and interconversion rate between α-ketoglutarate and glutamate were then determined by fitting ^{13}C enrichment curves to the kinetic model using the Levenberg−Marquardt method with standard deviations determined from the Jacobian matrix of the model.

Statistical Evaluation. All data are presented as mean ± standard deviation (mean ± SD). Comparison of intragroup data sets was performed with the Student's paired, two-tailed *t* test. Differences in mean values were considered statistically significant at a probability level of less than 5% ($p < 0.05$).

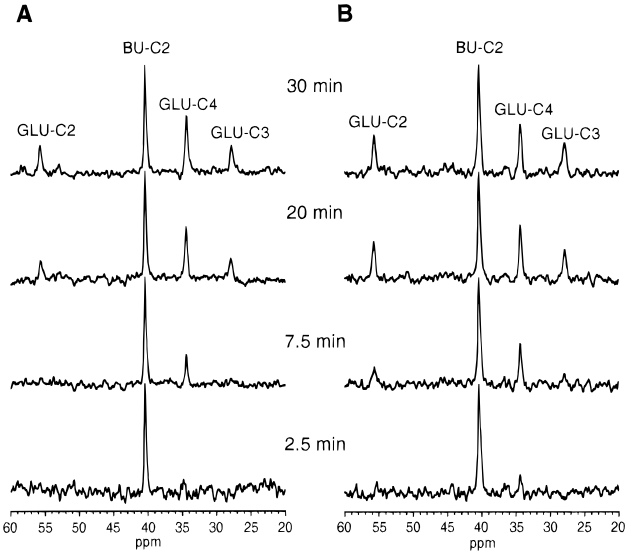

FIGURE 1: Effect of cytosolic redox state on sequential ^{13}C NMR spectra from isolated hearts. (A) Spectra from heart supplied with 2.5 mM [2-^{13}C]butyrate only; (B) spectra from heart supplied with 2.5 mM [2-^{13}C]butyrate and 2.5 mM unlabeled lactate. Peak assignments: GLU-C2, 2-carbon of glutamate; GLU-C3, 3-carbon of glutamate; GLU-C4, 4-carbon of glutamate; BU-C2, 2-carbon of butyrate. Heart perfused both butyrate and lactate show more rapid incorporation of ^{13}C into the 4- and 2-carbon sites of glutamate.

RESULTS

The evolution of the multiple ^{13}C enrichment sites in glutamate was monitored by sequential acquisition of ^{13}C NMR spectra from intact hearts. Representative changes in ^{13}C NMR spectra, reflecting the turnover of carbon isotope within the glutamate pool, are shown in Figure 1. Hearts perfused with both butyrate and lactate showed more rapid incorporation of ^{13}C into the 4- and 2-carbons of glutamate.

Enrichment curves for the 2- and 4-carbons of glutamate are shown in Figure 2, along with the results of the kinetic analysis by least-squares fitting of the model (solid line) to the data shown in the figure. In both groups, the correlation coefficient between the NMR data and the fitted curves was greater than 0.98. The obvious difference in enrichment rates between the two groups, as shown in Figure 2, was not accounted for by oxygen consumption rates which were similar at 25.3 ± 3.2 μmol min^{-1} (g dry weight)$^{-1}$ with butyrate alone and 24.7 ± 3.1 with butyrate plus lactate. Mechanical work, assessed by rate−pressure-product, was also similar between the two experimental groups: 14 700 ± 3100 beats·mmHg/min with butyrate alone and 17 000 ± 4300 with butyrate plus lactate (mean ± SD).

Experimentally measured parameters used for kinetic analysis are shown in Table 1. Lactate induced a redistribution of metabolites among the TCA cycle intermediates and amino acid pools, as was expected from the interaction of the malate−aspartate shuttle with the TCA cycle. Citrate level increased by more than 3-fold, while a shift in aspartate−oxaloacetate transamination reduced the aspartate concentration. Similar changes were also observed in rat heart when the transition was made from substrate free

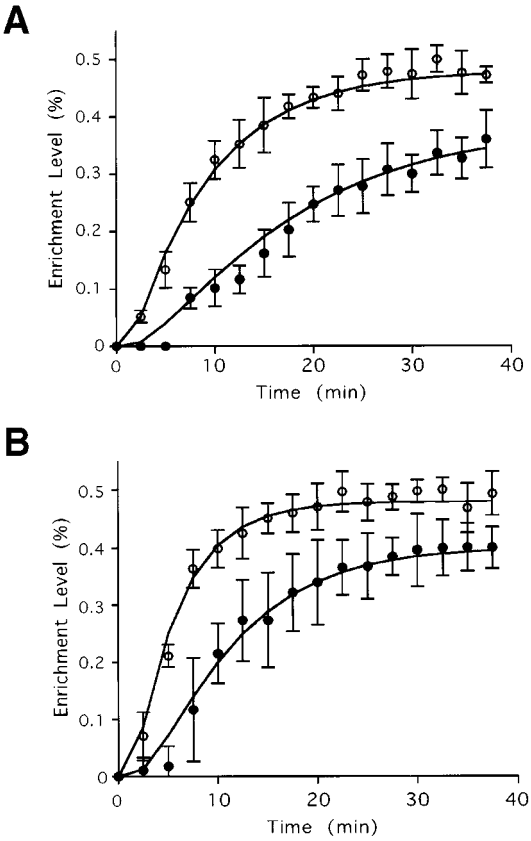

FIGURE 2: Time course of ^{13}C enrichment at different cytosolic redox states. ^{13}C NMR signal intensities are normalized to steady-state enrichment levels of glutamate (mean ± SD). Open circles: ^{13}C enrichment of glutamate at 4-carbon; closed circles: ^{13}C enrichment of glutamate at 2-carbon. The solid lines are the least-squares fittings of the kinetic model to the NMR data. (A) 2.5 mM [2-^{13}C]butyrate only; (B) 2.5 mM [2-^{13}C]butyrate + 2.5 mM unlabeled lactate.

Table 1: Parametric Data for Kinetic Analysis[a]

	butyrate	butyrate + lactate
^{13}C-enriched acetyl-CoA, F_c (%)	47.7 ± 2.0	48.0 ± 0.9
relative anaplerosis, y (%)	13.2 ± 1.5	10.5 ± 2.3
citrate (μmol/g dry weight)	0.95 ± 0.14	3.29 ± 0.59*
α-ketoglutarate (μmol/g dry weight)	0.32 ± 0.02	0.29 ± 0.02
glutamate (μmol/g dry weight)	24.22 ± 0.33	26.84 ± 2.12
aspartate (μmol/g dry weight)	2.09 ± 0.26	1.91 ± 0.21

[a] All data expressed as mean ± SEM. *p <0.05 as compared to perfusion with butyrate only.

Table 2: Output Data from Kinetic Analysis[a]

	butyrate	butyrate + lactate
V_{TCA}	9.66 ± 0.45	10.17 ± 0.29
F_1	3.11 ± 0.21	14.33 ± 1.97*

[a] Data shown are the TCA cycle flux (V_{TCA}) and the interconversion rate between α-ketoglutarate and glutamate (F_1). All data expressed in units of μmol min^{-1} (g dry wt)$^{-1}$ and as mean ± SD. *Significant difference between experimental groups at p <0.05.

perfusion to perfusion with glucose and insulin (Williamson et al., 1976).

Consistent with the observation of similar levels of mechanical work and respiratory rates, TCA cycle flux was also very similar between two groups, as shown in Table 2. However, the exchange rate between α-ketoglutarate and glutamate, shown as the parameter F_1 in Table 2, increased

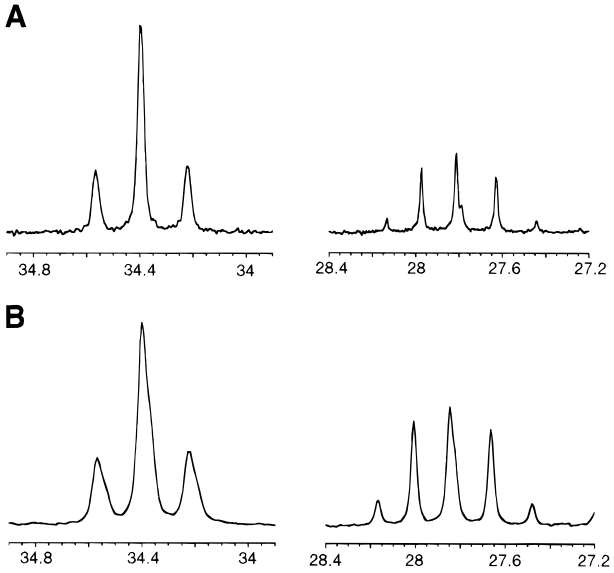

FIGURE 3: High resolution ^{13}C NMR spectra of glutamate from acid extracts. Multiplet structure of 3- and 4-carbon resonance of glutamate (GLU-C3 and GLU-C4) from heart perfused with [2-^{13}C]-butyrate alone (A) and [2-^{13}C] butyrate plus lactate (B). Note the similarity in multiplet structures denoting similar incorporation of label from butyrate into oxidative metabolites.

more than 4-fold. These data indicate increased metabolite transport across the mitochondrial membrane due to stimulated malate−aspartate shuttle activity in response to elevated cytosolic redox state.

As supportive data to demonstrate that the metabolic fate of the exogenous lactate did not alter the oxidation rate of butyrate, the ^{13}C enrichment of acetyl-CoA (F_c) and relative anaplerosis (y) are shown in Table 1. Both F_c and y values are similar in two groups. Note that the F_c values are less than 50% due to the fact that the single labeled [2-^{13}C]-butyrate gives rise to one labeled and one unlabeled acetyl-CoA molecules. Taking into consideration this partial enrichment of acetyl-CoA with [2-^{13}C]butyrate, over 95% of the acetyl-CoA entering the TCA cycle was from butyrate in both groups. Representative portions of the *in vitro* ^{13}C spectra from hearts in each group are shown in Figure 3 and demonstrate the similar multiplet structures in glutamate resonance from which the F_c values were determined. The similarity in these spectra demonstrates that the amount of butyrate oxidized by hearts with or without additional lactate was essentially the same. Therefore, hearts oxidizing ^{13}C-enriched butyrate did not utilize unlabeled exogenous lactate as a carbon source for oxidation. No signal was detected from ^{13}C-enriched glutamine in the ^{13}C NMR spectra of tissue extracts, indicating that glutamine synthase was not a significant pathway for consideration in the applied model.

To further confirm the effect of lactate, a heart was supplied with 2.5 mM unlabeled butyrate plus 2.5 mM [3-^{13}C]lactate. The ^{13}C NMR spectrum of acid extracts was obtained to document the relative utilization of butyrate and lactate for oxidative metabolism. The spectrum is shown in Figure 4 with the enlarged glutamate resonance at C2, C3, and C4 shown as insets. From these spectra, the complete lack of ^{13}C enrichment in glutamate beyond natural abundance and the absence of multiple structure within the glutamate resonance confirmed that lactate did not contribute to the formation of TCA cycle intermediates. Furthermore, the appearance of [3-^{13}C]alanine formed from the labeled

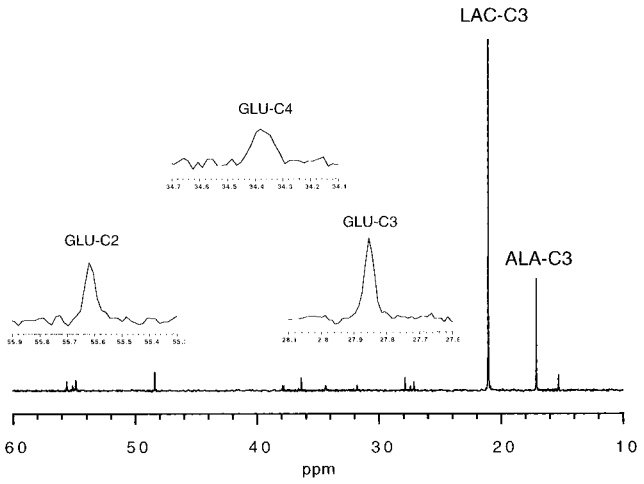

FIGURE 4: *In vitro* ^{13}C NMR spectrum of acid extract from heart perfused with unlabeled butyrate plus [3-^{13}C]lactate. Resonance signal arising from [3-^{13}C]alanine (ALA-C3) at 17 ppm demonstrates the conversion of lactate to pyruvate by lactate dehydrogenase. Other ^{13}C signals, besides exogenous [3-^{13}C]lactate (LAC-C3, 21 ppm), are at natural abundance level. The insets show enlarged glutamate resonance at the C2, C3, and C4 positions. The lack of multiplet structure within glutamate resonances indicates that ^{13}C-labeled lactate was not used as a carbon source for oxidative metabolism in the presence of butyrate.

lactate confirmed the effectiveness of the protocol to induce high redox state (NADH/NAD$^+$) via the conversion of lactate to pyruvate by lactate dehydrogenase.

DISCUSSION

In this study, a metabolic perturbation was used to induce differences in metabolite transport rates across the mitochondrial membrane, as reflected by the kinetics of ^{13}C turnover within the NMR detectable glutamate pool of intact, functioning hearts. Inducing an elevated cytosolic redox state with exogenous lactate caused an increase in the exchange rate of ^{13}C between the TCA cycle intermediates of the mitochondrial compartment with that of the largely cytosolic glutamate pool (Yu et al., 1995). The results of this work show directly, for the first time, that the exchange rates of metabolic intermediates between subcellular compartments responds to physiological perturbations of cell metabolism in intact functioning organs. In a previous study, our laboratory demonstrated that the interconversion of the TCA cycle intermediate, α-ketoglutarate, and glutamate involved a rate-determining process other than mere transaminase reaction. The current data demonstrate that this rate-determining process involves the transport of metabolic intermediates via the redox-sensitive malate−aspartate shuttle. Thus, dynamic-mode ^{13}C NMR spectroscopy of intact tissues is sensitive to chemical exchange and, more importantly, to the rate of metabolite transport between subcellular compartments.

It is necessary to point out that the use of inhibitors to explore the rate-limiting components is inappropriate, as inhibition will cause any step in the kinetic process, even rapid processes, to become rate-limiting. Therefore, our current protocol was designed to probe the physiological contributions of metabolite transport by stimulating, rather than inhibiting, this potential rate-determining step. Thus, by stimulating metabolite exchange across the mitochondrial membrane, via the influence of cytosolic redox state on the malate−aspartate shuttle activity, ^{13}C incorporation and turnover in the intramyocardial glutamate pool in intact, functioning rabbit heart were significantly affected (Figures 1 and 2). A least-squares fitting of a simple compartment model to these NMR data allowed the determination of both TCA cycle flux and the interconversion rate between α-ketoglutarate and glutamate, without introducing new rate limitations with the presence of inhibitory agents.

As reducing equivalents generated in the cytosol are shuttled into mitochondria for electron transfer, an unknown portion of oxygen will be consumed in oxidizing cytosolic reducing equivalents. Qualitatively, at a constant rate of ATP generation, increased flux through the malate−aspartate shuttle must be compensated by a decreased flux in the TCA cycle. Therefore, the use of oxygen consumption from known proportions of substrate utilization to calculate the TCA cycle flux, as per high resolution NMR analysis of tissue extracts, would be much less reliable in this case. With this important consideration and the previous finding that kinetic analysis determined with and without the incorporation of oxygen consumption as a constraint produced only a 10% discrepancy in measured TCA cycle flux (Yu et al., 1995), this study was performed without the constraint of measured oxygen consumption. Therefore, the least-squares fitting to the data presented here was dependent solely on isotope flux through the measured metabolite compartments.

The results of this study show that stimulated malate−aspartate shuttle activity induced a 4-fold increase in the interconversion rate between α-ketoglutarate and glutamate in hearts oxidizing the short chain fatty acid, butyrate. This activation occurred via elevated cytosolic redox state from the addition of exogenous lactate (Scholz et al., 1995). During perfusion with labeled lactate and unlabeled butyrate, NADH production via conversion of lactate to pyruvate was indicated from the production of [3-^{13}C]alanine. The [3-^{13}C]-alanine detected by ^{13}C NMR documented the reverse flux across the lactate dehydrogenase reaction. The absence of lactate oxidation in the presence of butyrate is consistent with the inhibition of pyruvate dehydrogenase activity by fatty acid oxidation (Dennis et al., 1979; Johnston & Lewandowski, 1991; Weiss et al., 1989). Therefore, the major effect of exogenous lactate was to increase cytosolic redox state (NADH/NAD$^+$). Under these conditions, the alanine transaminase (ATA) is likely to have caused some increase in the total transaminase flux (GOT + ATA), and the net enzymatic interconversion between α-ketoglutarate and glutamate then becomes even less rate-limiting for glutamate labeling relative to the net interconversion rate. The formation of alanine can also affect the activity of glutamine synthase. However, ^{13}C NMR spectra of tissue extracts in both groups showed no significant entry of ^{13}C into glutamine. Hence, glutamine synthase did not contribute to the observed isotope kinetics. Another minor consideration is that lactate also was likely to increase the cytosolic NADPH/NADP$^+$ ratio. As a cofactor for glutamate dehydrogenase, NADPH has the potential to shift the equilibrium of this reaction in other ograns, but the glutamate dehydrogenase is not the source of this isotope exchange in cardiac tissue (Brainard et al., 1986; Weiss et al., 1995).

The transaminase activity responsible for the exchange of label between α-ketoglutarate and glutamate follows simple double displacement reaction kinetics (Fahien & Strmecki,

1969). As was shown in previous experiments, the delivery of exogenous lactate to healthy, well-perfused myocardium does not exceed the pH buffering capacity of the cell, and thus pH was not a source of variation in enzyme activity in this study (Lewandowski et al., 1995). Therefore, without the allosteric regulation of the transaminase or changes in tissue pH, the observed acceleration in the interconversion of α-ketoglutarate and glutamate was achieved by driving the malate−aspartate shuttle at an elevated cytosolic redox potential with 2.5 mM exogenous lactate (Safer, 1975; Scholz et al., 1995).

In summary, the present ^{13}C NMR study addresses the potential to determine the rates of metabolite exchange across the mitochondrial membrane of intact functioning hearts. The results have shown directly that the NMR-observed ^{13}C turnover in the cardiac glutamate pool reflects adjustments in the metabolic communication between subcellular compartments of intact tissues in response to the metabolic state of the cell. These findings have important impact on future investigations of coordinated metabolic activities between the cytosolic and mitochondrial compartments of the cell in support of the physiological function of the whole organ. Certainly, studies examining the use of *in vivo* ^{13}C NMR spectroscopy for monitoring TCA cycle flux must carefully reconsider the often used assumption that the interconversion between α-ketoglutarate and glutamate is a negligible factor in the turnover of ^{13}C within the glutamate pool. More immediately, considerations of additional rate-determining steps among the processes contributing to carbon isotope turnover within the tissue glutamate pool open a new opportunity for current applications of ^{13}C NMR spectroscopy in the study of metabolic flux.

ACKNOWLEDGMENT

The authors thank Drs. K. F. LaNoue, T. J. Brady, and H. Taegtmeyer for their helpful comments during the preparation of the manuscript.

REFERENCES

Brainard, J. R., Hoekenga, D. E., & Hutson, J. Y. (1986) *Magn. Reson. Med. 3*, 673−684.

Chance, E. M., Seeholzer, S. H., Kobayashi, K., & Williamson, J. R. (1983) *J. Biol. Chem. 258*, 13785−13794.

Dennis, S. C., Padma, A., DeBuysere, M. S., & Olson, M. S. (1979) *J. Biol. Chem. 254*, 1252−1258.

Fahien, L. A., & Strmecki, M. (1969) *Arch. Biochem. Biophys. 130*, 468−477.

Johnston, D. L., & Lewandowski, E. D. (1991) *Circ. Res. 68*, 714−725.

LaNoue, K. F., & Williamson, J. R. (1971) *Metabolism 20*, 119−140.

LaNoue, K. F., Nicklas, W. J., & Williamson, J. R. (1970) *J. Biol. Chem. 245*, 102−111.

Lewandowski, E. D. (1992) *Circ. Res. 70*, 575−582.

Lewandowski, E. D., Chari, M. C., Roberts, R., Johnston, D. L. (1991) *Am. J. Physiol. 261*, H354−H363.

Lewandowski, E. D., Damico, L. A., White, L. T., & Yu, X. (1995) *Am. J. Physiol. 269*, H160−H168.

Malloy, C. R., Sherry, A. D., & Jeffrey, F. M. H. (1988) *J. Biol. Chem. 263*, 6964−6971.

Neely, J. R., Liebermeister, H., Battersby, E., & Morgan, H. (1967) *Am. J. Physiol. 212*, 804−814.

Randle, P. J., England, P. J., & Denton, R. M. (1970) *Biochem. J. 117*, 677−695.

Robitaille, P. M. L., Rath, D. P., Skinner, T. E., & Abduljalil, A. M. (1993) *Magn. Reson. Med. 30*, 262−266.

Safer, B. (1975) *Circ. Res. 37*, 527−533.

Scholz, T. D., Laughlin, M. R., Balaban, R. S., Kupriyanov, V. V., & Heineman, F. W. (1995) *Am. J. Physiol. 268*, H82−H91.

Weiss, R. G., Chacko, V. P., & Gerstenblith, G. (1989) *J. Mol. Cell. Cardiol. 21*, 469−478.

Weiss, R. G., Gloth, S. T., Kalil-Filho, R., Chacko, V. P., Stern, M. D., & Gerstenblith, G. (1992) *Circ. Res. 70*, 392−408.

Weiss, R. G., Stern, M. D., de Albuquerque, C. P., Vandegar, K., Chacko, V. P., & Gerstenblith, G. (1995) *Biochim. Biophys. Acta 1243*, 543−548.

Williamson, J. R., & Corkey, B. E. (1969) in *Methods in Enzymology* (Colowick, J. M., Ed.) Academic Press, pp 434−514, New York.

Williamson, J. R., Ford, C., Illingworth, J., & Safer, B. (1976) *Circ. Res. 38* (Suppl. I), I39−I51.

Yu, X., White L. T., Doumen, C., Damico, L. A., LaNoue, K. F., Alpert, N. M., & Lewandowski, E. D. (1995) *Biophys. J. 69*, 2090−2102.

BI960199L